

Gas gun driven dynamic fracture and fragmentation of Ti-6Al-4V cylinders at initial temperatures between 150 K and 750 K

David R. Jones, David J. Chapman, and Daniel E. Eakins

Citation: [AIP Conference Proceedings](#) **1793**, 100008 (2017); doi: 10.1063/1.4971633

View online: <https://doi.org/10.1063/1.4971633>

View Table of Contents: <http://aip.scitation.org/toc/apc/1793/1>

Published by the [American Institute of Physics](#)

Articles you may be interested in

[The fracture and fragmentation behaviour of additively manufactured stainless steel 316L](#)
AIP Conference Proceedings **1793**, 100002 (2017); 10.1063/1.4971627

[Deformation and failure of OFHC copper under high strain rate shear compression](#)
AIP Conference Proceedings **1793**, 100007 (2017); 10.1063/1.4971632

[On the influence of texture on spall evolution in the HCP materials Ti-6Al-4V and Zr](#)
AIP Conference Proceedings **1793**, 100010 (2017); 10.1063/1.4971635

[Non-equilibrium molecular dynamics simulations of spall in single crystal tantalum](#)
AIP Conference Proceedings **1793**, 070006 (2017); 10.1063/1.4971594

[Critical conditions for failure; stress levels, length scales, time scales](#)
AIP Conference Proceedings **1793**, 100006 (2017); 10.1063/1.4971631

[The stress and ballistic properties of granular materials](#)
AIP Conference Proceedings **1793**, 120023 (2017); 10.1063/1.4971705

AIP | Conference Proceedings

Get **30% off** all
print proceedings!

Enter Promotion Code **PDF30** at checkout



Gas Gun Driven Dynamic Fracture and Fragmentation of Ti-6Al-4V Cylinders at Initial Temperatures Between 150 K and 750 K

David R. Jones¹, David J. Chapman¹ and Daniel E. Eakins^{1,a)}

¹*Institute of Shock Physics, Imperial College London, Blackett Laboratory, Prince Consort Road, SW7 2BZ*

^{a)}Corresponding author: d.eakins@imperial.ac.uk

Abstract. We present a study on the dynamic fracture and fragmentation of Ti-6Al-4V cylinders at initial temperatures ranging from approximately 150 K to 750 K. Cylinders with an inner diameter of 50 mm and a wall thickness of 4 mm were driven into uniform axially-symmetric expansion at radial strain rates of 10^4 s^{-1} using the ogive-insert gas gun method. Diagnostics consisted of simultaneous high speed imaging and multiple points of laser velocimetry (PDV) along the length of the sample. The imaging and PDV provided a record of the expansion process, giving expansion velocity and the failure strain. Recovered fragments were examined with optical and scanning electron microscopy and electron backscatter diffraction techniques to determine the fracture mechanisms for each initial temperature. The failure strain (radial strain at first fracture) was observed to increase with temperature over the range tested, from 7.4 ± 5.2 percent at 158 K to 24.1 ± 2.4 percent at 724 K. In experiments from 158 K up to 609 K the fracture mechanism was found to be ductile tearing under mode II loading along the planes of maximum shear at 45° to the radius. At an initial cylinder temperature of 724 K the fracture mechanism transitioned to void nucleation and coalescence along adiabatic shear bands, again forming at 45° to the radial direction. The fragmentation toughness K_f was observed to also increase with temperature until the 724 K shot where there was a marked reduction, suggesting the formation of shear bands at high temperatures reduced the energy required to form fragments. The average value of K_f was $101 \pm 13 \text{ MPa m}^{1/2}$.

INTRODUCTION

Impact or shock loading of a material can result in its dynamic fracture and fragmentation. Here the term dynamic refers to the timescale over which the sample is loaded (or released) being comparable to that required for a wave to propagate around the sample. As failure can be influenced by a range of factors such as density, strength, distribution of flaws or nucleation sites in the sample [1] and strain rate experiments require careful consideration to ensure that as near to an equilibrium state as possible is reached under loading. Established loading techniques for studying fracture under tension such as the tensile split-Hopkinson pressure bar (SHPB) typically only load the sample from one end [2]. It is generally accepted that a SHPB test requires the load to traverse the sample three times to reach equilibrium [3]. At strain rates in excess of 10^3 s^{-1} significant plastic deformation and even fracture can occur well before this steady state is reached. One solution that can avoid these wave propagation limitations is to use an expanding ring or cylinder of the material of interest. The sample is uniformly loaded over the inner face, driving the ring or cylinder into radial expansion. At a time where the initial radial load has dissipated the sample continues to expand, with a hoop or circumferential tensile stress dominating. Under these conditions (prior to any localisation or failure) the entire azimuth of the sample is under a uniform stress and strain rate state. Three main methods are used to drive expansion: explosives, pulsed power and gas-guns. The two former methods have seen extensive use in studying different materials [4, 5, 6], stress state effects [7, 8, 9] and strain rate [10, 11]. The latter, gas-gun driven expansion, can be used to study the effect of initial sample temperature - not currently possible with the other drive methods. This is important as temperature not only affects a material's strength but can also influence the failure mechanisms available, such as a transition from brittle to ductile fracture or the formation of adiabatic shear bands. The work presented here covers the first results on the temperature dependent fracture and fragmentation of Ti-6Al-4V at strain rates on the order of 10^4 s^{-1} .

EXPERIMENTAL METHOD

A detailed description of the gas-gun expansion drive used here can be found in the authors' earlier work [12, 13, 14] and is a development of that used by Winter and Prestidge [15]. In brief, the sample material is machined into a cylinder. At the rear of this cylinder a steel ogive insert is installed and the cylinder assembly is then mounted concentrically to the end of the gas-gun barrel. The projectile is a solid polycarbonate cylinder with a concave leading face, and is launched into the target cylinder. The impact and resulting flow of the projectile around the ogive drives the cylinder into expansion from the inside face. Figure 1 shows a cross section of this process.

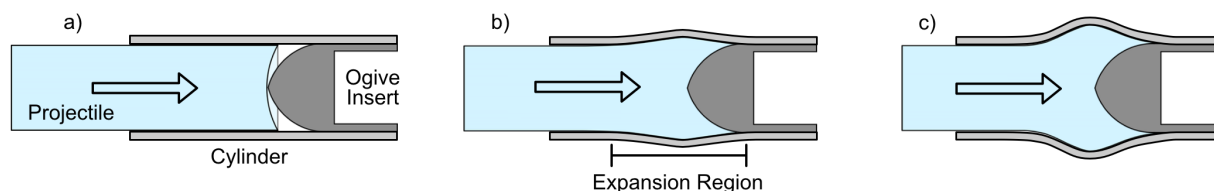


FIGURE 1. Ogive based gas-gun cylinder expansion. Projectile enters cylinder from left. a) At time of impact. b) & c) Later times where the projectile has driven the cylinder into radial expansion.

Cylinders were machined from solid rod stock Ti-6Al-4V (pct. by weight) with an inner diameter of 50 mm, a wall thickness of 4 mm and a length of 150 mm. Electron backscatter diffraction imaging revealed a grain structure of mostly equiaxed α phase titanium in a β matrix with an average grain size of around 5 μm and no preferential texture. The ogive inserts were machined from 4340 steel, with a long radius of 37.25 mm and a hollow at the rear 40 mm in diameter by 40 mm deep. For cooling, this hollow was sealed with an aluminium cap and a pressurised LN_2 feed was connected via a remotely operated valve. This is fully described by Jones *et al* [13]. For heating of the sample a macor (ceramic) spindle was affixed into the insert which supported a coil of 14 SWG nichrome wire. This resistive load was connected to a high current supply (maximum 62 A). The cylinder temperature was measured at multiple points along the length on the outer surface with thermocouples. The power supply was remotely operated via a LabVIEW interface, recording the current and voltage delivered to the heater as well as the thermocouple readings. The cylinder was mounted to the gas-gun via a sleeve with macor spacers to aid thermal isolation. The heating or cooling was only activated once the gas-gun target chamber had been evacuated to under 300 mTorr to avoid oxidation or ice formation on the cylinder. Projectiles were solid right cylinders of PC1000 polycarbonate with an outer diameter of 48 mm, a length of 150 mm and a concave leading face of radius 50 mm and were launched with a sabot.

Multiple channels of photon Doppler velocimetry (PDV [16]) were used. The cylinder expansion velocity was measured at four points along the length with a frequency-shifted PDV setup [17], using focusing probes with a large stand-off to avoid thermal damage. The zero-velocity beat frequency was $\sim 4.9 \text{ GHz}$ and the detectors were sampled with a Tektronix 71604 oscilloscope operating at 50 GS s^{-1} . The projectile velocity was measured with a single channel of homodyne PDV and a collimating probe. The velocity data was extracted using a sliding short-time Fourier transform as described by Dolan [18]. Two high speed imaging systems were used. A Vision Research Phantom v1610 observed the cylinder from one side along with a flash gun to provide front-lit high speed video at a rate of $\sim 250 \text{ kf s}^{-1}$. These images were used to determine the time of fracture and track crack growth along the sample. The other side of the cylinder was imaged with an Invisible Vision IVV UHSi 12/24 framing camera to provide high resolution silhouetted images at the same frame rate as the v1610. These images were processed to give the radial strain along the whole length of the cylinder and validated against the PDV data. The arrangement of the PDV probes and high speed imaging is shown in Figure 2. All oscilloscope and camera trigger signals and camera gating signals were recorded with a high bandwidth digitiser to allow synchronisation between diagnostics.

A momentum trap was used to capture cylinder fragments with minimal further damage. These recovered fragments were then cleaned to remove traces of polycarbonate, then weighed and measured. Fragments with features such as arrested fracture sites were sectioned, mounted and polished. For optical microscopy the polished faces were etched with Kroll's reagent, 2 % HF, 10 % HNO_3 and 88 % distilled water by volume for 30 s. Electron backscatter diffraction (EBSD) and scanning electron microscopy (SEM) were used to determine the fracture mechanism. EBSD post processing was performed using the open-source MTEX package for MATLAB [19].

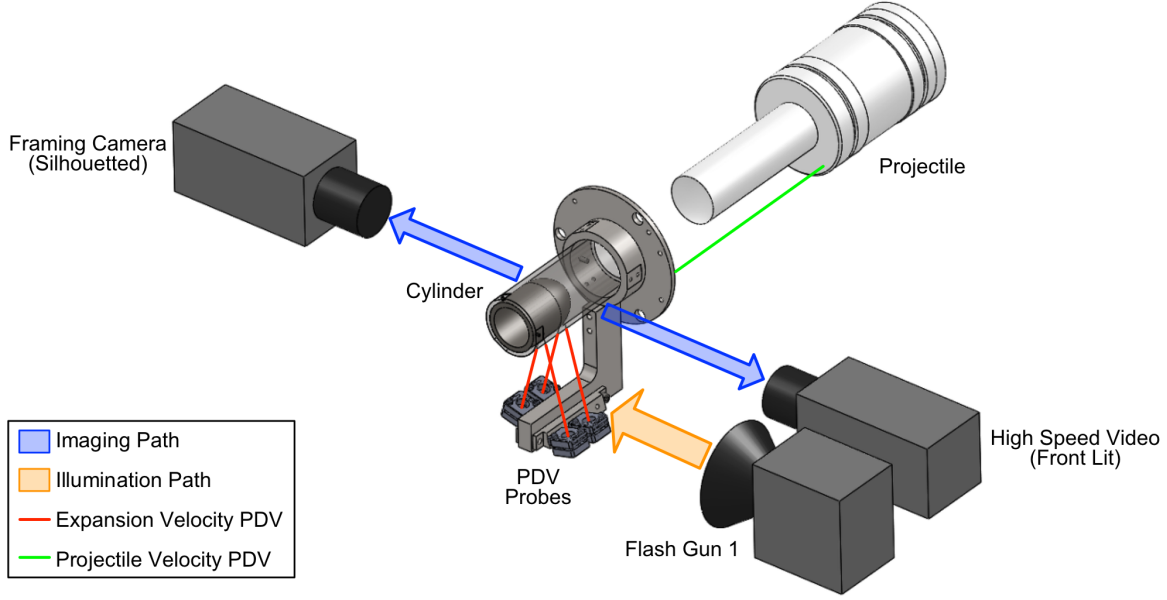


FIGURE 2. Arrangement of PDV probe paths and high speed imaging systems for an expanding cylinder experiment.

RESULTS AND DISCUSSION

A series of four cylinders were tested, each with a projectile velocity of $1000 \pm 5 \text{ m s}^{-1}$. A summary of the experiments is shown in Table 1. The temperature of each shot is given as the average temperature over the expansion region, the area between 80 mm and 120 mm from the cylinder entry. Radial strain rate is defined as:

$$\dot{\epsilon}_r(t) = \frac{v(t)}{r(t)}, \quad (1)$$

where $v(t)$ is the radial expansion velocity and $r(t)$ is the cylinder outer radius [20]. The strain at first failure is the radial strain accrued when the first fracture becomes visible on the cylinder outer surface. The relatively large error in some of these values is due to the frame rate of the high speed camera. It is not known at which point between two frames failure occurred and as such the error brackets the strain values from each frame. The final column, fragmentation toughness, is a parameter developed by Grady and Kipp [21, 22] related to the energy involved in dynamic fracture. For ductile fracture this is calculated with:

$$K_f = \frac{\rho c_0 \dot{\epsilon}}{\sqrt{12} N^{3/2}}, \quad (2)$$

where ρ is the density, c_0 is the bulk sound speed and N is the total number of cracks around the cylinder divided by the circumference, $N = N_{TOT}/2\pi r$. N_{TOT} has been extrapolated by doubling the visible fractures in the high speed video. Figure 3 plots the failure strain and K_f against temperature.

TABLE 1. Summary of the expanding cylinder experiments.

Shot Number	Average Temperature of Expansion Region (K)	Peak Radial Strain Rate ($\times 10^4 \text{ s}^{-1}$)	Radial Strain at First Fracture (%)	Fragmentation Toughness, K_f (MPa $\text{m}^{1/2}$)
1	158 ± 11	1.03 ± 0.01	7.4 ± 5.2	78 ± 8
2	290 ± 21	0.98 ± 0.01	18.2 ± 3.1	102 ± 13
3	609 ± 43	1.05 ± 0.01	12.5 ± 3.4	150 ± 23
4	724 ± 52	1.04 ± 0.01	24.1 ± 2.4	74 ± 7

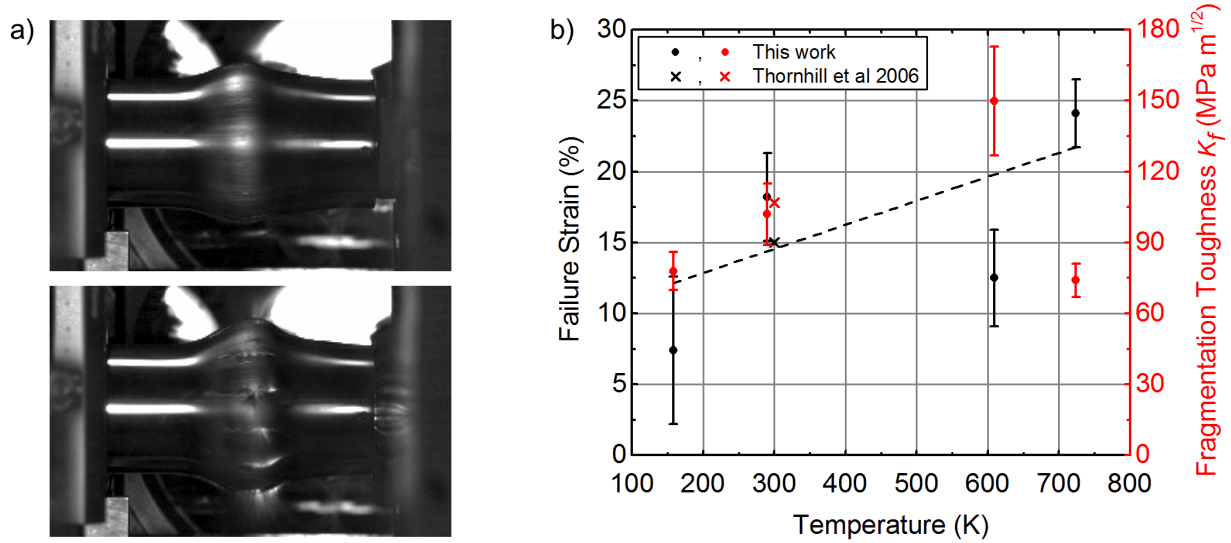


FIGURE 3. a) Two images from the 724 K shot, approximately 15 μ s apart showing deformation and appearance of fracture (projectile entered from left). b) Failure strain data and linear fit (black dots and dashed line) with fragmentation toughness (red dots) against the average temperature of the cylinder expansion region. Data from Thornhill *et al* [23] are also on Ti-6Al-4V.

It is clear that in general the failure strain increased with temperature, as expected from the increase in ductility and reduction in flow stress. The ambient temperature results were in good agreement with those of Thornhill *et al* [23], also on expanding Ti-6Al-4V cylinders. Fragmentation toughness increased with temperature, up to the shot at 724 K where there was a marked decrease. This experiment produced the highest number of fragments. One possible cause of this decrease was found by analysis of the recovered material. In the shots from 158 K to 609 K the fracture mechanism was through ductile tearing along the planes of maximum shear, at 45° to the radius (under mode II loading). This presented as parabolic dimples left on the fracture surfaces in the direction of the tearing as in Figure 4a. However, material from the 724 K shot was found to contain multiple adiabatic shear bands (ASBs) again at 45° to the radius. Here, instead of ductile tearing, fracture occurred through void nucleation and coalescence in these transformed bands. This was confirmed with SEM images of arrested fractures, showing bands of a much smaller grain size consistent with the melting and subsequent rapid quenching that occurs in an ASB. No evidence of these formations was observed in the lower temperature work. A typical arrested shear band and detail of the crack tip are shown in Figure 4b.

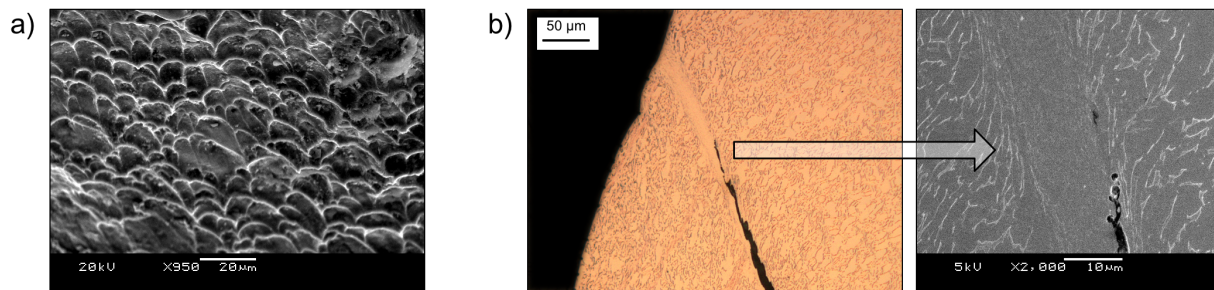


FIGURE 4. Recovered fragments. a) 609 K cylinder, SEM image of fracture surface showing parabolic dimples consistent with ductile tearing. b) 724 K cylinder, optical and SEM images showing fracture propagating along an adiabatic shear band.

It should be noted that the fragmentation toughness as defined in equation 2 is strictly applicable to ductile fracture and as such is not entirely suitable for use with the shot at 724 K. However, K_f is derived from the fragmentation *energy* in a similar way to the Griffith strain energy and stress intensity factor often used in quasi-static analyses are related [24]. The reduction in K_f at high temperature corresponds a decrease in the energy required for fracture and for a given

body more fragments will be produced. This could be related to the transition in fracture mechanism from ductile tearing to propagation along adiabatic shear bands, with the ASBs producing weakened sites for fracture to initiate. It was decided to plot ductile fragmentation toughness against temperature for consistency with other published results on gas-gun driven cylinders [25, 26, 27].

CONCLUSIONS

A series of experiments have been performed where Ti-6Al-4V cylinders were expanded using a gas-gun technique by Jones *et al* [13] at strain rates of $1 \times 10^4 \text{ s}^{-1}$ and temperatures from 158 K to 724 K. Laser velocimetry and high speed imaging were used to determine the failure strain and strain rate with analysis of the recovered fragments revealing the fracture mechanisms. Failure strain was found to generally increase with temperature, from 7.4 ± 5.2 percent at 158 K to 24.1 ± 2.4 percent at 724 K. The fragmentation toughness (and therefore fragmentation energy, where a greater energy required will result in less fragments per unit length) also increased, until the shot at 724 K where there was a marked reduction. Analysis of recovered fragments showed that at temperatures up to 609 K fracture occurred through ductile tearing along the planes of maximum shear (45° to the radius), whereas at 724 K fractures propagated along adiabatic shear bands by void nucleation and coalescence. This suggests that over a certain temperature ASBs can form, possibly under compression from the initial radial loading. These zones would then act as additional nucleation sites for failure, increasing the number of fractures and appearing as a reduction in fragmentation toughness / energy.

The fragmentation process is an inherently statistical event and as such confirmation of the conclusions proposed here requires further experimentation. Future work would concentrate on determining the temperature at which the adiabatic shear bands are activated and at what point during the expansion they form (either the initial radial compression during loading or the tensile hoop stress during expansion). This would be coupled with improved high speed imaging to reduce uncertainties in the failure strain and number of fractures.

ACKNOWLEDGMENTS

The authors and the Institute of Shock Physics gratefully acknowledge continued funding and support for the project from the Atomic Weapons Establishment (AWE plc) and Imperial College London. Samples were prepared by the Imperial Physics department workshop. The Phantom v1610 high speed camera was kindly supplied by Vision Research. Dr Terry Jun of the Imperial Materials department is thanked for his assistance with the fragment preparation and microscopy.

REFERENCES

- [1] N. F. Mott, *Proc. R. Soc. A* **189**, 300–308 (1947).
- [2] J. Harding, E. O. Wood, and J. D. Campbell, *J. Mech. Eng. Sci.* **2**, 88–96 (1960).
- [3] E. D. H. Davies and S. C. Hunter, *J. Mech. Phys. Sol.* **11**, 155–179 (1963).
- [4] R. W. Gurney, *The Initial Velocities of Fragments from Bombs, Shell, Grenades*, BRL-405 (Ballistic Research Laboratories, Aberdeen, MD, 1943).
- [5] R. H. Warnes, T. A. Duffey, R. R. Karpp, and A. E. Carden, *Improved Technique for Determining Dynamic Material Properties using the Expanding Ring*, LA-UR-80-1543 (Los Alamos Scientific Laboratory, Los Alamos, NM, 1980).
- [6] W. D. Reid and B. E. Walsh, *J. Phys. IV France* **1**, 3–3 (1991).
- [7] D. M. Goto, R. Becker, T. J. Orzechowski, H. K. Springer, A. J. Sunwoo, and C. K. Syn, *Int. J. Imp. Eng.* **35**, 1547–1556 (2008).
- [8] H. Zhang and K. Ravi-Chandar, *Int. J. Fract.* **150**, 3–36 (2008).
- [9] D. R. Jones, D. E. Eakins, A. S. Savinykh, and S. V. Razorenov, *DYMAT 2012 EPJ Web of Conferences* **26** (2012).
- [10] D. E. Grady and D. A. Benson, *Exp. Mech.* **23**, 393–400 (1983).
- [11] N. S. Al-Maliky and D. J. Parry, *Meas. Sci. Tech.* **7**, 746–752 (1996).
- [12] D. R. Jones, D. E. Eakins, P. J. Hazell, D. J. Chapman, and G. J. Appleby-Thomas, *AIP Conf. Proc.* **1426**, 1141–1144 (2012).
- [13] D. R. Jones, D. J. Chapman, and D. E. Eakins, *J. Appl. Phys.* **114**, p. 173508 (2013).

- [14] D. R. Jones, D. J. Chapman, and D. E. Eakins, *J. Phys.: Conf. Ser.* **500**, p. 112037 (2014).
- [15] R. E. Winter and H. G. Prestidge, *J. Mat. Sci.* **13**, 1835–1837 (1978).
- [16] O. T. Strand, D. R. Goosman, C. Martinez, T. L. Whitworth, and W. W. Kuhlow, *Rev. Sci. Instr.* **77**, p. 083108 (2006).
- [17] P. Mercier, J. Bénier, P. A. Frugier, A. Sollier, M. R. Le Gloahec, E. Lescoute, J. P. Cuq-Lelandais, M. Boustie, T. De Resseguier, and A. Claverie, *AIP Conf. Proc.* **1195**, p. 581 (2009).
- [18] D. H. Dolan, *Rev. Sci. Instr.* **81**, p. 053905 (2010).
- [19] F. Bachmann, R. Hielscher, and H. Schaeben, *Solid State Phenomena* **160**, 63–68 (2010).
- [20] C. R. Hoggatt and R. F. Recht, *Exp. Mech.* **9**, 441–448 (1969).
- [21] D. E. Grady and M. E. Kipp, *Int. J. Imp. Eng.* **20**, 293–308 (1997).
- [22] D. E. Grady, *Fragmentation of rings and shells: The Legacy of N.F. Mott* (Springer, 2006).
- [23] T. F. Thornhill, L. C. Chhabildas, and T. J. Vogler, *AIP Conf. Proc.* **845**, 666–669 (2006).
- [24] A. A. Griffith, *Phil. Trans. R. Soc. A* **221**, 163–198 (1921).
- [25] T. F. Thornhill, W. D. Reinhart, L. C. Chhabildas, D. E. Grady, and L. T. Wilson, *AIP Conf. Proc.* **620**, 515–518 (2002).
- [26] T. J. Vogler, T. F. Thornhill, W. D. Reinhart, L. C. Chhabildas, D. E. Grady, L. T. Wilson, O. A. Hurricane, and A. Sunwoo, *Int. J. Imp. Eng.* **29**, 735–746 (2003).
- [27] S. M. Stirk and R. E. Winter, *AIP Conf. Proc.* **1426**, 949–952 (2012).